Science Fund of the Republic of Serbia

Grant Agreement No.: 7750824

Call: IDEJE

Hybrid Integrated Satellite and Terrestrial Access Network

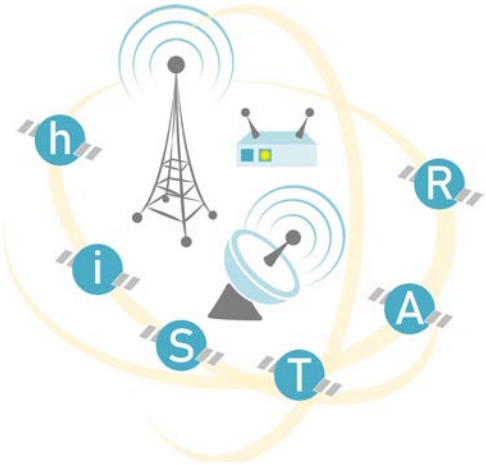

D6.1: Channel emulator for 5G/satcom signals

Work package	WP 6
Subactivity	T6.1
Due date	15/1/2025
Submission date	15/1/2025
Deliverable lead	SEE
Version	1.0
Authors	Haris Turkmanović, Zoran Čiča, Predrag Ivaniš
Reviewers	Goran Đorđević, Dejan Drajić

Document Revision History

Version	Date	Description of change	List of contributor(s)
V0.1	05/01/2025	1st version of D6.1	Predrag Ivaniš
V0.2	08/01/2025	2nd version of D6.1	Zoran Čiča
V0.3	13/01/2025	3rd version of D6.1	Haris Turkmanović
V1.0	15/01/2025	The final deliverable	

COPYRIGHT NOTICE

ACKNOWLEDGMENT

Science Fund of the Republic of Serbia

This deliverable has been written in the context of hi-STAR project who has received funding from the Science Fund of the Republic of Serbia, Programme IDEJE under grant agreement n° 7750284.

EXECUTIVE SUMMARY

The hi-STAR project addresses one of the most critical challenges for the next generation wireless networks, which is integration of non-terrestrial networks with terrestrial 5G network. The general objective of the WP6 is to integrate a ITCU developed in WP4 with satellite and 5G modems developed in WP3 into the HUT module. As a first step in this process, it is necessary to develop the accurate channel emulator for 5G/satcom signal propagation.

This deliverable is a result of the work done in the context of WP6 Subactivity 6.1 (Analysis of channel models for 5G/satcom signal propagation). We explain the channel model for satellite-to-ground communication links at the physical layer. It is used to calculate the outage probability as a function of the signal-to-noise ratio thresholds, for various propagation scenarios. Given the payload size calculation, discussion regarding headers and information about modulation and code formats (MODCOD), we obtained relation to payload size from application layer that fits short frame given the used MODCOD for satellite links. These results will be used in framework to estimate performance of intelligent controller in HUT.

TABLE OF CONTENTS

LIST OF FIGURES

LIST OF TABLES

ABBREVIATIONS

ACF	**Autocorrelation Function**
ACM	**Adaptive Coding and Modulation**
AM	**Acknowledge Mode**
AWGN	**Additive White Gaussian Channel**
DVB	**Digital Video Broadcasting**
EIRP	**Effective Isotropic Radiated Power**
FEC	**Forward Error Correction**
FER	**Frame Error Rate**
FSPL	**Free-Space Path Loss**
LDPC	**Low-Density Parity-Check**
LEO	**Low-Earth-Orbit**
LOS	**Line of Sight**
PDCP	**Packet Data Convergence Protocol**
QoS	**Quality of Service**
RLC	**Radio Link Control**
RLE	**Return Link Encapsulation**
SDAP	**Service Data Adaptation Protocol**
SDU	**Service Data Unit**
SNR	**Signal-to-Noise Ratio**
TCP	**Transmission Control Protocol**
TM	**Transparent Mode**
UDP	**User Datagram Protocol**
UM	**Unacknowledge Mode**
WP	**Work Package**
FTP	**Frame Transmission Period**

CTP **Complete Transfer Time**

SECTION 1 - INTRODUCTION

Channel model represents and analyzes channel on physical layer. However, structured data (frames) are transferred over channel. It is important to connect channel model i.e. physical layer to frames that belong to upper layers to establish complete simulator that is capable of observing and simulating transmission including all communication layers. One of the main goals of this deliverable is to connect channel model from physical layer to higher layers or more precisely to frames that are actually transmitted over the emulated channel. Thus, analysis of frame structure is provided along with the made assumptions. Based on results from channel model and frame structure analysis, payload size and number of frames that can be sent in some time period is determined. Based on this information, it is possible to devise a framework that enables simulation of frames over considered channel whose model is represented in this deliverable.

The Deliverable D6.1 summarizes the initial work carried within WP6 subtask T.6.1. In the above subtask we have investigated possibility to develop an accurate channel emulator for 5G/satcom communication links. The terrestrial channel is modeled based on the two-wave with diffuse power (TWDP) diffuse model, which is characteristic for the millimeter waves, and Nakagami-*m* fading model for microwave transmission. The satellite communication is modeled by using Shadowed-Rician propagation. The aforementioned channel models were developed and tested in WP2, while the integration into simulation framework was conducted in WP4 subtask T.4.1. In this deliverable, previously developed channel models at the physical layer are used to calculate the outage probability as a function of the signal-to-noise ratio thresholds. Then, we obtained relation to payload size from application layer that fits short frame given the used MODCOD for satellite links. These results will be used in framework to obtain optimal data transfer, and we will have a good reference to estimate performance of intelligent controller in HUT

This deliverable is structured as follows: In Section 2 we briefly explain channel model at the physical layer, the overview of the MODCODs is given, and the outage probability expression is derived. In Section 3 we describe the process of adding headers at each of the communication layers to payload created at application layer, and we calculate payload size for each MODCOD. In Section 4 we describe the simulation framework. Section 5 concludes the document.

SECTION 2 – CHANNEL MODEL AND MODCODS

2.1. CHANNEL MODEL

As explained in Deliverable 4.1, the instantaneous SNR at satellite-terrestrial link is defined as following

$$\gamma(t) = \bar{\gamma} \times |h(t)|^2,$$

where $\bar{\gamma}$ denotes the average SNR ant the receiver and $h(t)$ is the time varying gain on the link.

The average SNR is determined by the parameters of the system, and for the LEO satellite system the logarithm representation of the average SNR is determined by [2]

$$\bar{\gamma}\,[\text{dB}] = EIRP\,[\text{dB}] - n_{SD}*10\log10(4\pi d_{SD} f_0/c) - L_A[\text{dB}] - L_{add}[\text{dB}] + G\,[\text{dB}] - 10\log10(kT_S B), \quad (1)$$

where EIRP denotes effective isotropic radiated power, L_A denotes atmospheric losses due to oxygen and water, L_{add} denotes and the other losses (polarization mismatch, antenna misalignment), G denotes antenna gains. The second term at the right side of Eq. (1) corresponds to free-space path loss (FSPL), where d_{SD} denotes the distance between the satellite and receiver at the destination, n_{SD} denotes the corresponding path loss factor, f_0 denotes the carrier frequency at the satellite-terrestrial link, and c=3×10^8 m/s denotes the speed of light. The last term in the above expression corresponds to the noise level, where k=1.38×10^{-23} J/K denotes the Boltzmann constant, T_S denotes the temperature of the system, and B denotes the channel bandwidth.

We can easily rewrite Eq. (1) in the form that corresponds to the representation from Deliverable 4.1, i.e.

$$\bar{\gamma}_1\,[\text{dB}] = P_S\,[\text{dB}] - n_{SD}*10\log_{10}(d_{SD}) - 10\log10(\sigma^2), \quad (2)$$

where transmitted power P_S takes into account power-related parameters same for all system users

$$P_S\,[\text{dB}] = \text{EIRP}\,[\text{dB}] - n_{SD}*10\log_{10}(4\pi f_0/c) - L_A[\text{dB}] - L_{add}[\text{dB}] + \text{G}\,[\text{dB}], \quad (3)$$

the second term in (2) takes into account variable parameters of FSPL, and the third factor corresponds to the power of the noise at the receiver. Furthermore d_{SD} = H/sin(θ), where H is the satellite altitude and θ is the corresponding elevation angle.

The satellite-terrestrial downlink operates in Ku-band, and typical values for EIRP, L_A, f_0, G, T_S, and B for active LEO satellite systems can be found in [2, 3]. For the parameters presented in Table 2, that corresponds to OneWeb satellite system, we obtain $\bar{\gamma} = 11.3$ dB [2, 4, 5].

Table 1. System and simulation parameters

system parameters	*value*	simulation parameters	*value*
EIRP	34.6 dBW	P_S	17.53 dBW
L_A	1 dB	σ_n^2	-89 dBm
L_{add}	0.5 dB	n_{SD}	2

G	10.5 dB	H	1200 km
T_s	363 K	θ	40°
B	250 MHz	L	25 km
f_0	11 GHz		

On the other hand, the time-varying channel gain $h(t)$ depends on the fading properties in the channel. In the previous reports (D2.3 and D4.1), it was shown that the time-varying gain can be adequately described by using Shadowed-Ricean fading [6] in the case when the user terminal is located in the rural environment, while Gamma-Gamma fading model [7] can be more adequate in the user terminal is located in the urban environment. It our previously published papers [8] and [9] we proposed a simulator that that correctly captures the first and second-order statistics of the random processes related to the multipath and shadowing effects for these fading models, respectively. For most use cases, the satellite link will be used in a rural environment (mountains, deserts, oceans,), and in the rest of the deliverable we will concentrate to Shadowed-Ricean fading that is widely accepted to describe the links between the LEO satellites and terrestrial users [10].

As explained in [5], using the method illustrated in Figure 1, we are able to generate the temporally correlated time series $h(n)$ that correspond to the channel gains of the satellite-terrestrial links and the channel gain of the terrestrial link:

- We apply the method based on autoregressive models [11] to generate the time series $x(n)$ that describes the multipath component. It corresponds to the complex Gaussian random process with a Rayleigh distributed envelope. In the case of isotropic scattering, the normalized autocorrelation function is given by $R_r(\tau) = J_0(2\pi f_{Dm}\tau)$, where f_{Dm} denotes the maximum Doppler shift for the multipath component (we assume f_{Dm} = 100 Hz).
- The first step is repeated to generate an time series $y(n)$, independent from $x(n)$, with the Rayleigh distributed envelope and ACF $R_s(\tau) = J_0(2\pi f_{Ds}\tau)$, where f_{Ds} denotes the maximum Doppler shift for the shadowing (which is usually $f_{Ds} << f_{Dm}$, while in our simulations we chose f_{Ds} = 1Hz]).
- Based on the rejection/acceptance technique, described in [12], we have generated temporally uncorrelated time series $z_{un}(n)$ with Nakagami distribution. Using the properties of the second order statistics described in [13], the rank matching method proposed in [14] is applied to reorder the samples in that process according to the previously generated reference $y(n)$. The resulting time series $z(n)$ corresponds to the time-varying LOS component that has an envelope with Nakagami distribution (as in $z_{un}(n)$) and normalized ACF $R_s(\tau) = J_0(2\pi f_{Ds}\tau)$ (as in $y(n)$).
- Channel gains for the satellite-terrestrial link are obtained by using the expression $h(n)=x(n)+z(n)$.

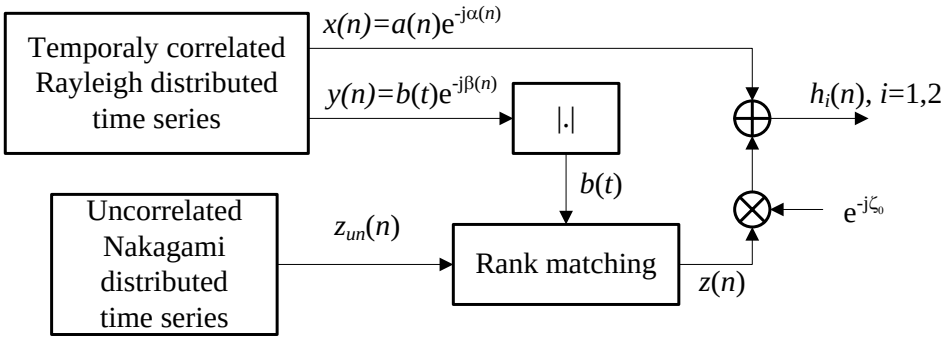

Figure 1. The simulator of the Nakagami-*m* and shadowed Rice channel gains with desired first and second-order statistics.

Finally, the *n*-th sample of the SNR waveform at the receiver is determined by

$$\gamma(n) = \overline{\gamma}\left|h(n)\right|^2. \tag{4}$$

Figure 2 shows the instantaneous SNRs at the receiver, where the simulator for the shadowed Rice fading is applied to determine the samples of the channel gains. Typical channel conditions for the satellite-terrestrial channel are described by the level of shadowing included in the model, and we distinguish low, average and heavy shadowing with the corresponding values presented in Table 2 (as determined in [6]).

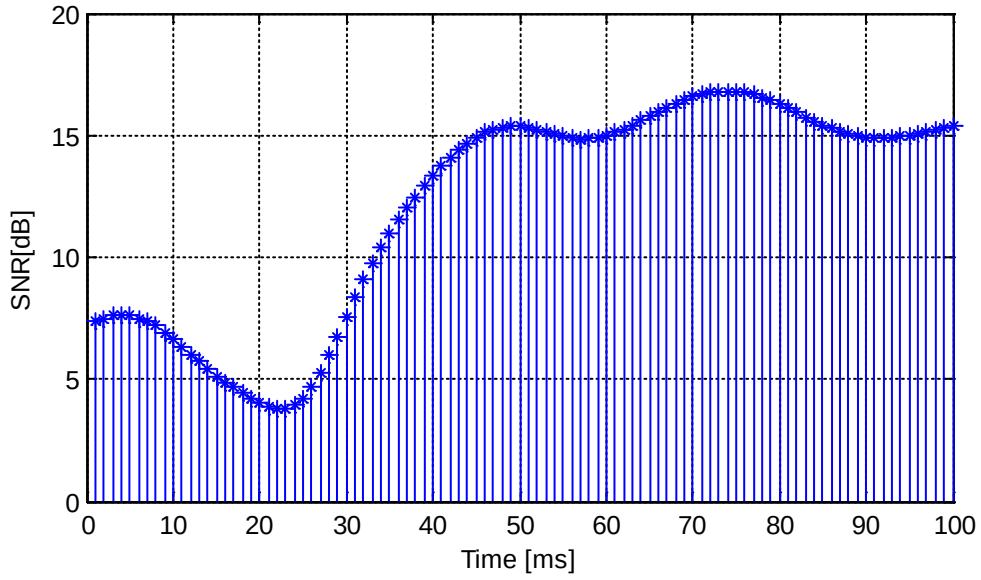

Figure 2a. The discrete waveforms of the instantaneous SNR – the light shadowing.

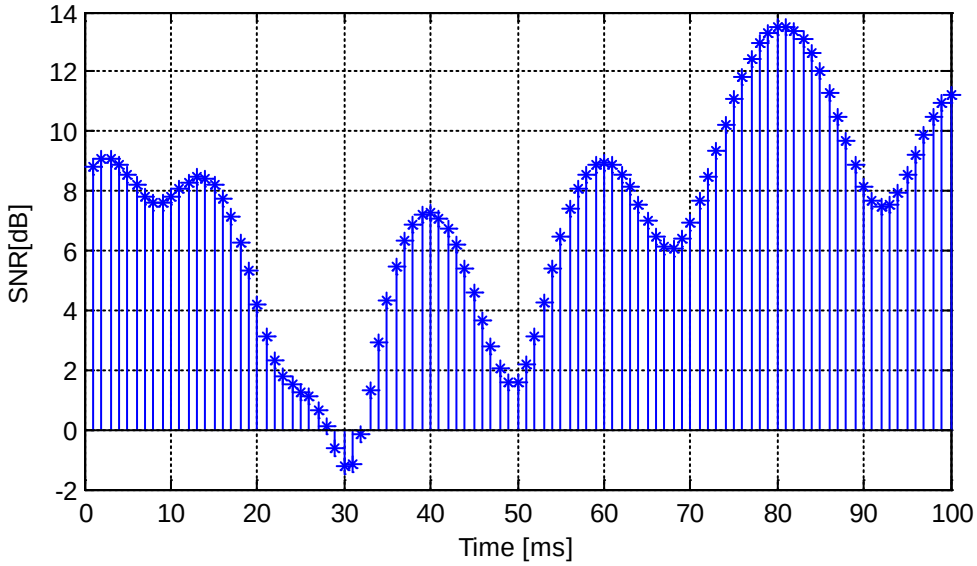

Figure 2b. The discrete waveforms of the instantaneous SNR – the average shadowing.

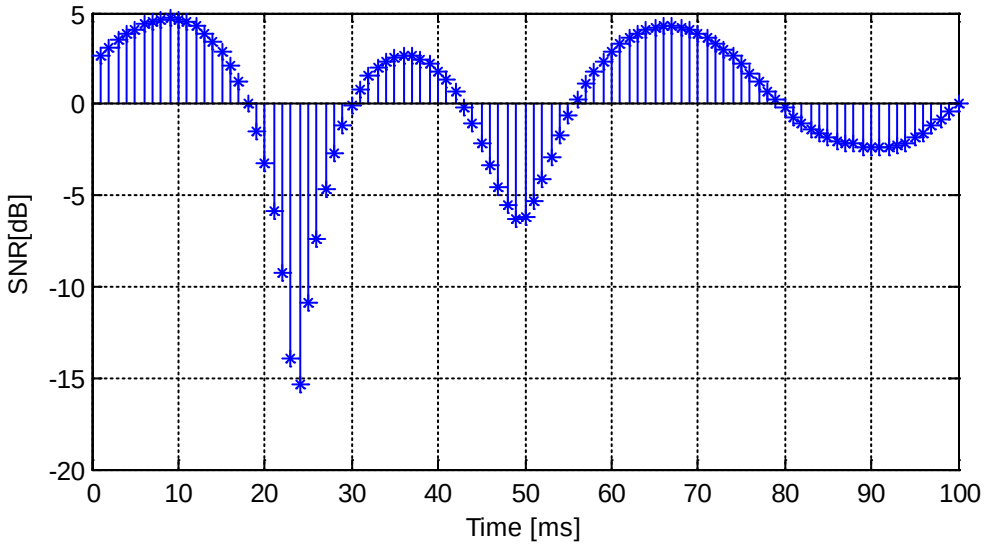

Figure 2c. The discrete waveforms of the instantaneous SNR – the heavy shadowing.

Table 1. Satellite channel parameters for different propagation scenarios.

Propagation scenario	b_0	Ω	m
Infrequent low shadowing	0.158	1.29	19.4
Average shadowing	0.126	0.835	10.1
Frequent heavy shadowing	0.063	0.000897	0.739

The instantaneous SNR presented in Figure 2 corresponds to carrier-to-noise ratio (C/N), as defined in [2, 4, 15, 16]. However, interference from the other satellites and other communication systems often represents a limiting factor in the downlink of LEO systems. The exact modelling of the interference is out of the scope of this deliverable, and the corresponding analysis can be found in [15], [16]. Similar as in those papers, we will introduce carrier-to-noise plus interference ratio, denoted by C/(N+I). However, we will simplify analysis assuming certain values of the interference to noise ratio, denoted by I/N. Using typical values of that parameter, we will present the relevant numerical results for a LEO satellite system.

2.2. MODULATION AND CODING MODES

We assume that the end-user could establish connection through several LEO satellites and terrestrial base station that supports 5G millimeter wave communication. Similar as Deliverable 4.1, we only consider downstream traffic direction from the network core to the end user. Each radio link supports adaptive coding and modulation (ACM) technique meaning that the sender of information adopts the data rate to the channel state information.

In this deliverable, we concentrate on satellite-terrestrial where the data transmission is performed based on DVB-S2X protocol. As the data transmission is more sensitive to propagation delay, we will assume that short frames of length 16200 bits are used. The corresponding MODCOD couples (modulation format, code rate) provide spectral efficiencies 0.1b/Hz/s - 3.56b/s/Hz, as shown in Table 3 (we consider that level of tolerated transmission unreliability is 10^{-5}) [1].

Our simulation is based on the SNR waveforms generated in the previous section. For the *n*-th waveform sample, if *SNR*(*n*)>9.9 dB, we chose the MODCOD with highest spectral efficiency M_i that satisfy *SNR*(*n*)> $T(M_i)$. This way, the highest spectral efficiency is provided in every time instant. The chosen MODCOD provides FER<10^{-5} after LDPC decoding, and FER<10^{-7} after BCH decoding. Certainly, the number of delivered packets on the IP layer depends on the achieved spectral efficiency. On the other hand, if *SNR*(*n*)<9.9 dB, neither one MODCOD can provide the required reliability (FER<10^{-5}), and the transmission in that discrete moment is considered to be unsuccessful. In such a case, the corresponding packets have to be retransmitted.

Table 3 : MODCODs used for system evaluation.

MODCOD 2		
Modulation	M_i[b/s/Hz]	$T(M_i)$ [dB]
BPSK-S 1/5	0.1	-9.9
BPSK-S 11/45	0.12	-8.3
BPSK 1/5	0.2	-6.1
BPSK 4/15	0.27	-4.9
BPSK 1/3	0.33	-3.72

QPSK 11/45	0.49	-2.5
QPSK 4/15	0.53	-2.24
QPSK 14/45	0.62	-1.46
QPSK 7/15	0.93	0.6
QPSK 8/15	1.07	1.45
QPSK 32/45	1.42	3.66
8PSK 8/15	1.60	4.71
8PSK 26/45	1.73	5.52
16APSK 7/15	1.87	5.99
16APSK 8/15	2.13	6.93
16APSK 26/45	2.31	7.66
16APSK 3/5	2.40	8.1
16APSK 32/45	2.84	9.81
32APSK 2/3	3.33	11.41
32APSK 32/45	3.56	12.18

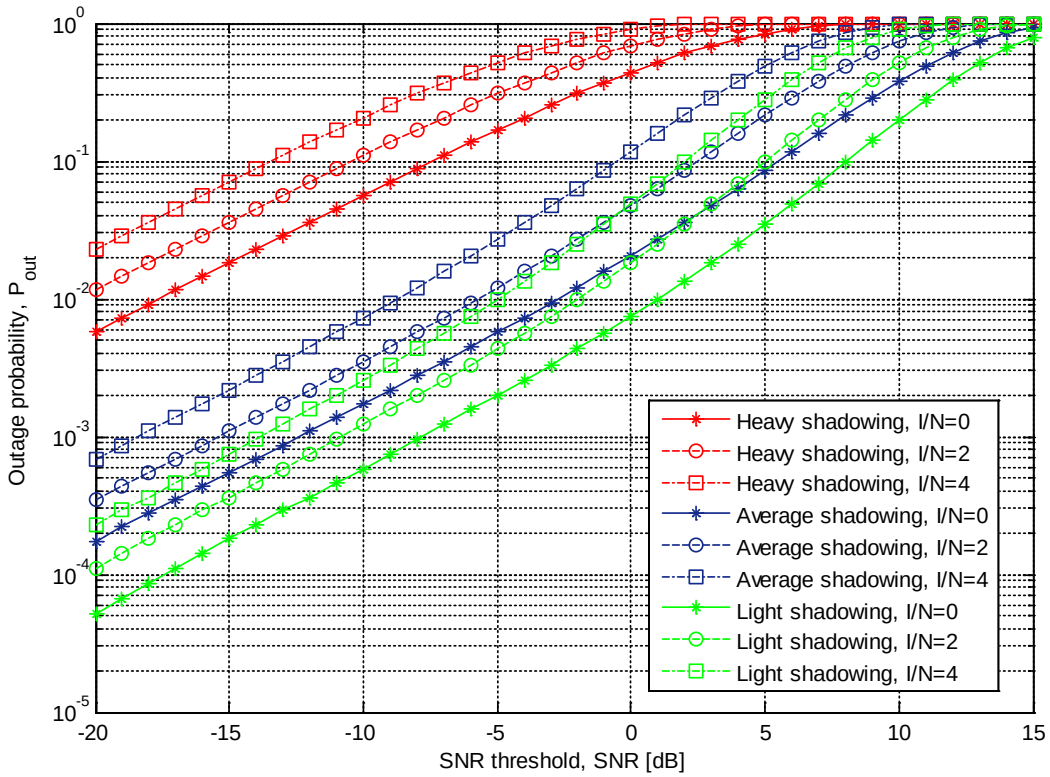

Figure 3. Outage probability vs. SNR threshold for various propagation scenarios.

In Figure 7, we show the outage probability (denoted by P_{out}) as a function of the SNR thresholds, for various propagation scenarios. The numerical results are presented for the case

when only AWGN is present in the channel (I/N=0), and for the cases when interference is two or four times larger than the noise (I/N=2 and I/N=4). The theoretical results are obtained by using Eq. (31) from paper [4], and the Monte Carlo simulation results are estimated based on 10^7 samples and basic principles of simulation of communications systems [17].

In accordance with the expectations, the outage probability increases with the increase of the SNR threshold. The outage probability decreases for better propagation conditions in satellite-terrestrial link S-D, as well as for the lower level of interference.

As previously stated, short frames in DVB-S2X protocol cannot be transmitted reliably if signal-to-noise ratio is lower than -9.9 dB. Therefore, we are interested in outage probability for that SNR. According to the numerical results presented in Figure 3, in the case of light shadowing and in the absence of interference, $P_{out}=6\times10^{-4}$ if SNR=-9.9dB. On the other hand, in the case of heavy shadowing and interference four times stronger than AWGN, Pout=2×10^{-1} for the same signal-to-noise ratio level.

SECTION 3 – HIGHER LAYERS

Application creates content (payload) that needs to be sent. To that payload, headers of layers below application layer are added (transport, network and data-link layer). Finally, based on selected MODCOD, it is determined how many message bits can be sent inside the short frame of 16200 bits. By message bits we assume payload with added headers (transport, network and data-link headers).

Regarding the transport layer, we have selected UDP (User Datagram Protocol) protocol because it provides more flexibility in our own research regarding multipath solutions at transport layer. Also, in this way we can support multimedia sessions that are typically based on UDP. However, the same calculations and approach can be applied to TCP (Transmission Control Protocol) protocol used for transmissions/sessions over emulated channel. UDP header is short, only 8 bytes long, i.e. 32 bits long. Figure 4 shows UDP header structure. Explanations of header fields can be found in RFC 768.

Source port (16b)	Destination port (16b)
UDP length (16b)	Checksum (16b)

Figure 4. UDP Header.

At the network layer, IP protocol needs to be used. There are IPv6 and IPv4 versions. IPv4 basic header is 20 bytes long, i.e. 160 bits long. IPv6 basic header is 40 bytes long, i.e. 320 bits long. In our tests, we use IPv4 header, but the same approach and calculations can be used for IPv6 case. Figure 5 shows IPv4 basic header structure. Explanations of header fields can be found in RFC 791.

<table>
<tr><td>Version (4b)</td><td>IHL (4b)</td><td>Type of Service (8b)</td><td colspan="2">Total Length (16b)</td></tr>
<tr><td colspan="3">Identification (16b)</td><td>Flags (3b)</td><td>Fragment Offset (13b)</td></tr>
<tr><td colspan="2">TTL (8b)</td><td>Protocol (8b)</td><td colspan="2">Header Chekcsum (16b)</td></tr>
<tr><td colspan="5">Source IP address (32b)</td></tr>
<tr><td colspan="5">Destination IP address (32b)</td></tr>
</table>

Figure 5. IPv4 Header.

Data-link layer depends on link type - satellite or 5G (terrestrial). In case of 5G, SDAP (Service Data Adaptation Protocol) is responsible to accept IP packets. SDAP header might not be needed and omitted in case of only one QoS flow. Otherwise, SDAP header is 1 byte long, i.e. 8 bits long. We will assume that SDAP header is added. Then, PDCP (Packet Data Convergence Protocol) would add its own header - 16 bits header along with 32 bits for integrity check. Also, PDCP can perform header compression where headers from upper layers are compressed. This

feature can be disabled. Below PDCP, there is RLC (Radio Link Control), where three modes of operation are defined:

- TM (Transparent Mode),
- UM (Unacknowledged Mode),
- AM (Acknowledge Mode).

TM mode does not add header. UM mode is suitable for UDP sessions, where AM mode is suitable for TCP sessions because it supports feedback with ACKs and NACs. In UM mode, header depends on size of data, does it contain complete RLC SDU (Service Data Unit) or not. Similar is with AM mode where size of header depends on configured size of sequence number (12 or 18 bits), and if segment offset field is present in header or not. We will in our initial research stages assume UM mode that is in line with our UDP selection at transport layer. Also, we will assume that complete RLC SDU is contained in one packet at RLC layer, thus, there is 1 byte, i.e. 8 bits in RLC header. In total 5G (SDAP, PDCP and RLC) would add 8 bytes, i.e. 64 bits in total.

In the case of satellite link, we have assumed RLE (Return Link Encapsulation) protocol. There are different cases that impact on overall data link layer header size. However, we assume that data fits in one frame and optional header fields are not used, Thus, we assume that header is 2 bytes long, i.e. 16 bits long.

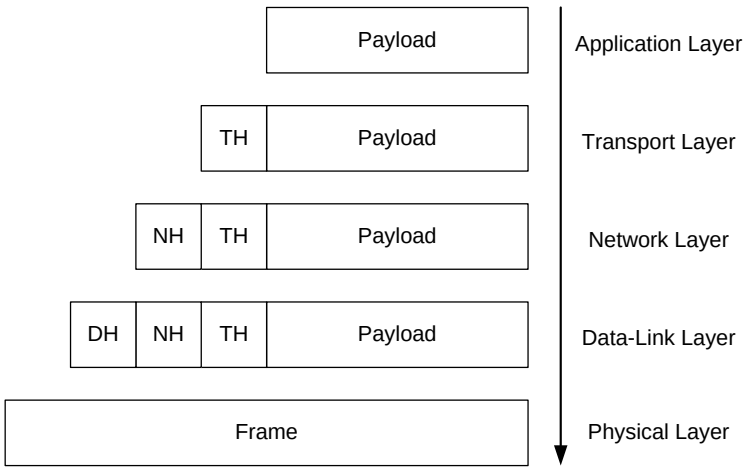

Figure 6. Adding headers to final frame.

Figure 6 illustrates the process of adding headers at each of the communication layers to payload created at application layer. Note that final frame structure actually considers packet from data-link layer as message that is protected using LDPC/BCH coding. Based on that figure we can calculate payload size for each MODCOD case according to following equations:

$$R = (PAYLOAD + TH + NH + DH) / FS \Rightarrow PAYLOAD = FS*R - (TH + NH + DH) \quad (5)$$

Used notation is the following: FS - frame size in bits, R - code rate, PAYLOAD - size of payload in bits, TH - transport layer header size in bits, NH - network layer header size in bits, DH - data link layer header size n bits. In our case TH is equal to 32 bits, and NH is equal to 160 bits. DH for satellite link is 16 bits, while for 5G it is 64 bits under our assumptions. FS in the case of satellite link is 16200 bits.

Table 4 : Satellite link payload size and number of frames for channel size 10Mhz and 10 ms SNR measurements.

Satellite link		
Modulation	Payload size [b]	Number of frames
BPSK-S 1/5	3032	0.617284
BPSK-S 11/45	3752	0.740741
BPSK 1/5	3032	1.234568
BPSK 4/15	4320	1.666667
BPSK 1/3	5192	2.037037
QPSK 11/45	3752	3.024691
QPSK 4/15	4320	3.271605
QPSK 14/45	4832	3.82716
QPSK 7/15	7352	5.740741
QPSK 8/15	8432	6.604938
QPSK 32/45	11312	8.765432
8PSK 8/15	8432	9.876543
8PSK 26/45	9152	10.67901
16APSK 7/15	7352	11.54321
16APSK 8/15	8432	13.14815
16APSK 26/45	9152	14.25926
16APSK 3/5	9512	14.81481
16APSK 32/45	11312	17.53086
32APSK 2/3	10592	20.55556
32APSK 32/45	11312	21.97531

Given the aforementioned payload size calculation, discussion regarding headers and results presented in Table 3, it is possible to create Table 4 that contains relation to payload size from application layer that fits short frame given the used MODCOD for satellite links. The same approach can be applied for 5G terrestrial links. Also, based on spectral efficiency and channel size, it is possible to calculate the number of frames that can be sent during the observed period (measurement time slot) for which SNR measurement stands:

$$NF = M*CS*T/FS \quad (6)$$

Used notation is the following: NF - number of frames, M - spectral efficiency in b/s/Hz, CS - channel size in Hz, T is measurement time slot in s, FS - frame size in bits. Table 4 shows example of calculation results for channel size of 10MHz, and measurement time slot of 10ms. When NF is not integer value, floor function should be used. However, one can start sending the frame even if frame sending would spread over next measurement time slot. If in the next measurement slot, MODCOD is same or better, frame would be transferred successfully (of course, taking into account FER), otherwise frame would not be transferred successfully (transfer would certainly fail). In our case we will assume sending only the number of frames that can be

sent completely in the time slot. But after these tests, we will consider also the case of starting a frame transfer in one slot that will be completed in the next time slot.

In the previous case, we observed measurement time slot as transfer time slot. Transfer time slot is the speed of devices to adjust to new MODCOD for transfer. In general case, transfer time slot can be greater than measurement time slot. Of course, it is easy to extend calculations in (6) to such case. In this extended case, T would represent transfer time slot, and M would represent the worst (minimal) M value from all the measurements in transfer time slot.

Calculations presented in the previous and this section will be used in framework to obtain optimal data transfer. This will be referencing value to compare with, when predicting methods based on machine learning are included where MODCODs to use will be predicted for future transfer time slots. In this way, we will have good a reference to estimate performance of intelligent controller in HUT.

SECTION 4 - FRAMEWORK

To fully understand how channel-related functionalities are implemented within a simulation framework, as well as the key principles driving them, it is essential to first presents the overall working principles of the simulation framework and its main software components. The simulation framework is designed as a distributed solution comprising three primary software components deployed across two different platforms. The components are as follows:

1. **H**ybrid **U**ser **T**erminal (HUT)
   This component is responsible for configuring other simulation components based on various system configuration parameters. It also generates data and monitors communication across all components within the system.

2. Transmitter/Receiver
   This component handles receiving data from the HUT, analyzing it, forwarding it to the channel, and subsequently receiving data back from the channel. It then returns the data, along with relevant statistical information, to the HUT.

3. Channel
   This component implements the logic required to emulate channel behavior.

The HUT is implemented as a software solution developed using Qt and deployed on a PC, whereas the Transmitter/Receiver and Channel are also implemented as software solutions but are deployed on dedicated FPGA boards.

Within the simulation framework, data is exchanged between components as encapsulated binary-format messages. These messages are created at the application layer and then passed down to the lower network layers, where headers are added at each layer, as described in the previous section. At the application layer, the payload itself consists of two parts: a header and the payload data. The application-layer header is specifically designed to support essential functionalities, such as monitoring packet transfers within the simulation, detecting packet losses, evaluating packet size and performance, and other related tasks. The current framework includes six fields in the application-layer header, each 4 bytes in size, adding a total of 136 bits. While this additional header slightly reduces the effective user data bandwidth in simulator, it significantly enhances the robustness and functionality of the framework. Therefore, message payload size presented in Table 4 for satellite link should be decreased for 136 bits in case this simulation framework is used. The structure of the data message is illustrated in Figure 7.

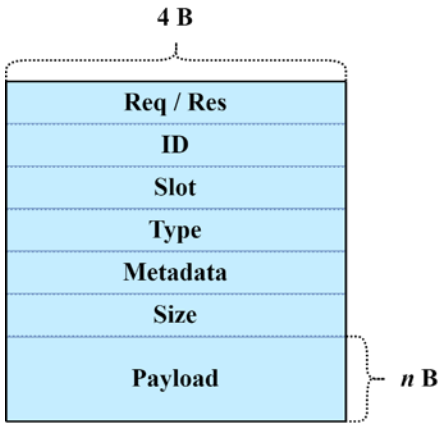

Figure 7. Data message structure

A key aspect of channel functionality is the ability to achieve different communication rates based on the selected modulation and channel bandwidth. The first section provides spectral efficiencies for each modulation, allowing the calculation of communication rates for each modulation type when the channel size is known. For satellite and terrestrial links, channel sizes are defined by standards and typically fall within the range of tens of MHz. However, these standard channel sizes cannot be fully supported within the simulation framework due to performance bottlenecks caused by various software components. Benchmarking of the simulation environment has revealed that the maximum channel size achievable within the framework is approximately 70 kHz. Although this value is significantly smaller than standard channel sizes, it does not impact the simulation's functional accuracy. To better maps real-world performance scenarios within a simulation framework, all time-related information should be appropriately scaled.

The simulation framework is designed to facilitate data transfer and emulate the behavior of real terrestrial or satellite links. As input data that should be transfer over simulator, it uses either a file or a specified amount of dummy data to be transmitted over the preconfigured network. These data are divided into smaller chunks, with the size determined by the applied modulation scheme. Each chunk is then processed by adding the appropriate headers at each network layer and incorporating error correction bits. The final message size, before being transmitted from the HUT, is 16200 bits. The simulation framework periodically transmits frames from the HUT through the Transmitter/Receiver, adhering to a Frame Transition Period (FTP). The FTP is configured to achieve communication rate of the selected modulation and to maximize the number of frames that can be transmitted during the measurement period, which corresponds to the SNR measurement interval (slot). Therefore, before start transmission of frames it is important to configure FTP value in simulation time to achieve desired FTP for corresponding slot.

During the simulation, the SNR measurement period will remain fixed. For the analysis relevant to this project, it is assumed that between two SNR measurements, an integer number of frames will always be transmitted using the FTP that is configured to achieve baud rate that correspond to the modulation selected for that slot. Consequently, during a single simulation slot, a different number of frames will be generated depending on the selected modulation. This is illustrated in Figure 8.

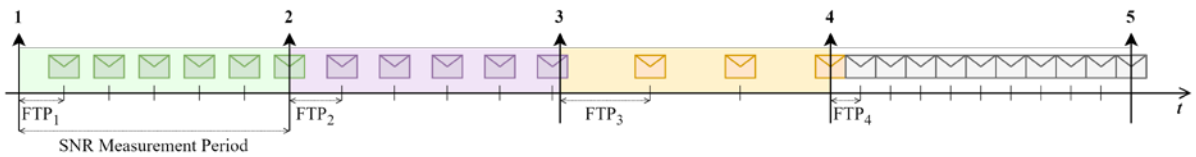

Figure 8. Frame transmission over time

The number of frames corresponding to a single slot for various modulation schemes is outlined in Table 4. Generally, this value can be a floating-point number. However, within the simulation framework, these values are rounded to the nearest integer to simplify processing logic. As a result, if a frame transmission begins and an SNR measurement occurs during the transfer, the updated measurement results will only take effect after the frame's transmission is complete.

Table 5 presents the final payload size within the simulation framework, the Frame Transition Period (FTP), the number of frames per slot, and the Complete Transfer Time (CTP) required to transmit 1 Mb of data. These calculations are based on the spectral efficiencies for satellite links specified in Table 3, using a channel size of 10 MHz and an SNR measurement interval of 10 ms. According to Table 4, the maximum achievable communication rate for the selected modulation range with a 10 MHz channel size is approximately 35 Mbps, enabling the transmission of up to 22 frames during a single SNR measurement interval. The values in Table 5 are scaled to simulation time, which assumes a channel size of 70 kHz and a maximum communication rate of approximately 225 kbps. This results in a time scaling ratio of roughly 155 between real-world values and simulation values.

Table 5: Satellite link payload size, frame transmission period and complete transfer time for 1Mb of data in simulation time domain.

Satellite link				
Modulation	Payload size [b]	FTP [s]	Number of frames during single slot	CTP for 1Mb data [s]
BPSK-S 1/5	2896	2.314286	1	799.1318
BPSK-S 11/45	3616	1.928571	1	533.3439
BPSK 1/5	2896	1.157143	1	399.5659
BPSK 4/15	4184	0.857143	2	204.8621
BPSK 1/3	5056	0.701299	2	138.7062
QPSK 11/45	3616	0.472303	3	130.6148
QPSK 4/15	4184	0.436658	3	104.3637
QPSK 14/45	4696	0.373272	4	79.4872
QPSK 7/15	7216	0.248848	6	34.48558
QPSK 8/15	8296	0.216288	7	26.07141
QPSK 32/45	11176	0.162978	9	14.58284
8PSK 8/15	8296	0.144643	10	17.43525
8PSK 26/45	9016	0.133774	11	14.83737
16APSK 7/15	7216	0.123759	12	17.15058

16APSK 8/15	8296	0.108652	13	13.0969
16APSK 26/45	9016	0.100186	14	11.11197
16APSK 3/5	9376	0.096429	15	10.28462
16APSK 32/45	11176	0.081489	18	7.291422
32APSK 2/3	10456	0.069498	21	6.646717
32APSK 32/45	11176	0.065008	22	5.816752

Besides communication rate, which is an important channel characteristic, another important channel characteristic is the Frame rejection mechanism. Figure 9 illustrates frame rejection mechanism implemented inside simulator.

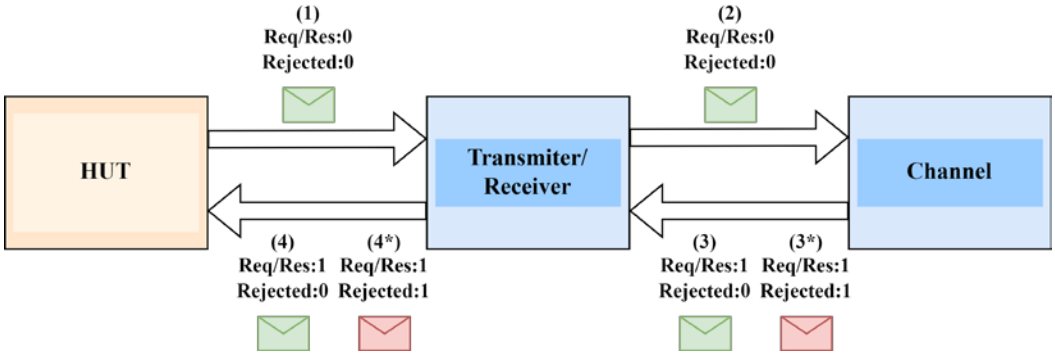

Figure 9. Frame rejection mechanism

In the simulator, a data message represents a frame analogous to those used in real communication systems. The binary structure of this message includes a header containing two key fields relevant to the rejection mechanism: **Req/Res** and **Rejected**. The **Req/Res** field, when set to zero, indicates that the message is a request generated by the HUT. A value of one indicates that a response message. Initially, both fields are set to zero, and the HUT begins transmitting messages to the Transmitter/Receiver component with predefined FTP (1). Upon receiving the message, the Transmitter/Receiver component processes it without modifying these fields. After processing, the message is forwarded to the Channel component (2). The Channel component simulates real-world channel behavior and incorporates a rejection mechanism. This mechanism, based on a predefined probability that corresponds to the channel's characteristics, determines whether the message is rejected. If the message is not rejected, only the Req/Res field is updated in the message content, and the message is routed back to the HUT (3)(4). However, if the message is rejected, the Req/Res field is set to one, the Rejected field is also set to one, and the message is then transmitted back to the HUT (3*) (4*).

SECTION 5 CONCLUSIONS

In this deliverable we presented a channel emulator for 5G/satcom signals. We used the channel model for satellite-to-ground communication links at the physical layer to determine the corresponding outage probability. For various parameters related to higher network layers, we obtained relation to payload size from application layer that fits short frame given the used MODCOD for satellite links. We used these results in the developed framework to estimate performance of intelligent controller in HUT.

REFERENCES

[1] ETSI TR 102 376-1 V1.2.1 (2015-11), Digital Video Broadcasting (DVB); Implementation guidelines for the second-generation system for Broadcasting, Interactive Services, News Gathering and other broadband satellite applications; Part 1: DVB-S2.

[2] D. Rozenvasser, K. Shulakova, “Estimation of the Starlink Global Satellite System Capacity“, in *Proc. of the 12th International Conference on Applied Innovation in IT (ICAIIT 2024)*, Kothen, Germany, 9. March 2023, pp. 55-59.

[3] Del Portillo, I; Cameron B. G.; Crawley, E. F. A technical comparison of three low earth orbit satellite constellation systems to provide global broadband. *Acta Astronautica*, **2019**, *159*, 123-135. DOI: 10.1016/j.actaastro.2019.03.040.

[4] S. Xia, Q. Jiang, C. Zou and G. Li, "Beam Coverage Comparison of LEO Satellite Systems Based on User Diversification," *IEEE Access*, vol. 7, pp. 181656-181667, 2019

[5] P. Ivaniš, J. Milojković, V. Blagojević, and S. Brkić. "Capacity Analysis of Hybrid Satellite–Terrestrial Systems with Selection Relaying" *Entropy*, vol. 26, no. 5: paper no. 419, May 2024.

[6] A. Abdi, W. C. Lau, M.-S. Alouini and M. Kaveh, “A new simple model for land mobile satellite channels: first- and second-order statistics,” *IEEE Trans. Wireless Commun.*, vol. 2, pp. 519-528, May 2003.

[7] I. M. Kostic, “MGF for Gamma-Shadowed Ricean fading Channel,” *European Trans. on Telecommun.* vol. 19, pp. 155-159, Mar. 2008.

[8] P. Ivaniš, V. Blagojević, and G. Đorđević, “The method of generating shadowed Ricean fading with desired statistical properties”, in *Proc INFOTEH XXII*, Jahorina, BiH, March 2023.

[9] G. T. Djordjevic, D. Milić, P. Ivaniš, I. Radojković, "A Simulation Model for Generating Time Variant Gamma-Shadowed Ricean Fading Samples", in *Proc 32th Telecommunications Forum (TELFOR 2024)*, November 26-27, 2024, Belgrade, Serbia, pp. 1-4.

[10] G. Pan, J. Ye, J. An and M. -S. Alouini, "Latency Versus Reliability in LEO Mega-Constellations: Terrestrial, Aerial, or Space Relay?," *IEEE Transactions on Mobile Computing*, vol. 22, no. 9, pp. 5330-5345.

[11] Baddour K. E.; Beaulieu, N. C. Autoregressive modeling for fading channel simulation. *IEEE Trans. Wireless Commun*., 2005, 4, 1650-1662. DOI: 10.1109/TWC.2005.850327.

[12] Papoulis A.; Pillai, S. U. *Probability Random Variables and Stochastic Processes*, McGraw-Hill, Boston, Mass, USA, 4th ed., 2002.

[13] Yacoub, M.D.; Bautista, J.E.V.; Guerra de Rezende Guedes, L. On higher order statistics of the Nakagami-m distribution. *IEEE Trans. Veh. Technol*., 1999, 48, 790–794. DOI: 10.1109/25.764995.

[14] Silveira Santos Filho, J. C.; Yacoub M. D.; Fraidenraich, G. A Simple Accurate Method for Generating Autocorrelated Nakagami-m Envelope Sequences. *IEEE Commun. Letters*, 2007, 11, 231-233.

[15] J. M. Gongora-Torres, C. Vargas-Rosales, A. Aragón-Zavala and R. Villalpando-Hernandez, "Link Budget Analysis for LEO Satellites Based on the Statistics of the Elevation Angle," *IEEE Access*, vol. 10, pp. 14518-14528, 2022.

[16] E. Kang, W. Shin, Y. Park, Y. B. Park, J. Kim and H. Choo, "Link Budget Analysis of Low Earth Orbit Satellites Considering Antenna Patterns and Wave Propagation in Interference Situations," in *Proc 2022 International Symposium on Antennas and Propagation (ISAP)*, Sydney, Australia, 2022, pp. 511-512,

[17] Jeruchim, M.C.; Balaban, P.; Shanmugan, K.S. *Simulation of Communication Systems: Modeling, Methodology and Techniques*; Springer Science & Business Media: Berlin, Germany, 2006.